Research Square

Preprints are preliminary reports that have not undergone peer review.
They should not be considered conclusive, used to inform clinical practice,
or referenced by the media as validated information.

A Multi-Stage Optimized Framework for Fundus Image Classification in Diabetic Retinopathy

Usharani Bhimavarapu
Koneru Lakshmaiah Education Foundation
K Rama Krishnaiah
R K College of Engineering
J. Sivavara Prasad
Lakireddy Bali Reddy College of Engineering
Sk Hasane Ahammad
Koneru Lakshmaiah Education Foundation
Mustafa SirElkhatim
mustafa1979@rsu.edu.sd
Red Sea University
Wallaaldin Eltayeb
Koneru Lakshmaiah Education Foundation

Article

Keywords: Grey Wolf Optimization, Support Vector Machine, Artificial Bee Colony, Differential Evolution, adaptive encircling, spiral search

Posted Date: October 8th, 2026

DOI: https://doi.org/10.21203/rs.3.rs-10730236/v1

License: This work is licensed under a Creative Commons Attribution 4.0 International License.
Read Full License

Additional Declarations: No competing interests reported.

A Multi-Stage Optimized Framework for Fundus Image Classification in Diabetic Retinopathy

[1]Usharani Bhimavarapu, **[2]K Rama Krishnaiah ,[3]J. Sivavara Prasad, [1]Sk Hasane Ahammad, [4]Mustafa SirElkhatim & [5]Wallaaldin Eltayeb**

[1]Department of CSE, Koneru Lakshmaiah Education Foundation, Guntur, India-522302
E-mail: ushareddy@kluniversity.in, ahammadklu@gmail.com
[2]Department of CSE, R K College of Engineering, Kethanakonda, India
E-mail: kondraguntark@gmail.com
[3]Professor, Department of EEE, Lakireddy Bali Reddy College of Engineering, Mylavaram.
E-mail: janapatisivavaraprasad@gmail.com
[4]Department of Chemical Engineering, Red Sea University, Port Sudan, 3315, Sudan
E-mail: mustafa1979@rsu.edu.sd
[5]Department of EEE, Koneru Lakshmaiah Education Foundation, Vaddeswaram, 522302, India
E-mail: walla129@gmail.com
Correspondence Author: ahammadklu@gmail.com, mustafa1979@rsu.edu.sd

Abstract: Diabetic retinopathy (DR) is a progressive retinal disease and is a major contributor to irreversible blindness in diabetic patients globally. Recognizing retinal lesions early and correctly will be vital to preventing vision impairment and for timely clinical intervention. This study introduces an intelligent optimization-based framework for automated detection of diabetic retinopathy, where Improved Grey Wolf Optimization (IGWO) is used to preprocess the retinal images, Improved Whale Optimization Algorithm (IWOA) to segment lesions in the retinal images, Improved Artificial Bee Colony (IABC) to select features from the retinal images, and an Improved Fuzzy Support Vector Machine (IFSVM) to detect the diabetic retina. First, the images of the retina undergo enhancement for image contrast, reduction of noise and illumination variations with IGWO. The improved images are then segmented applying IWOA for precise estimation of the lesion regions. The image segments of the lesions are then used to extract comprehensive colour, texture and shape features, which are then optimized using IABC to remove redundant information while retaining highly discriminative features. Lastly, the optimized feature subset is classified by using the proposed IFSVM. The preprocessing stage of IGWO had a PSNR of 38.64 dB, SSIM of 0.986, MSE of 0.0042, entropy of 7.82, contrast improvement index of 2.06 and processing time of 0.78 s. The IWOA segmentation algorithm proposed in this paper achieved a Dice coefficient of 98.42%, IoU of 96.89%, sensitivity of 98.51%, specificity of 98.83%, precision of 98.46%, and overall segmentation accuracy of 98.68%. The IABC algorithm has only 82 informative features (with a feature reduction of 65.6%), and only 6.41s to optimize. The proposed Improved Fuzzy Support Vector Machine demonstrated superior classification accuracy (98.55%), precision (98.48%), recall (98.51%), F1-score (98.49%) and AUC (99.02%) compared to the rest of the conventional machine learning and deep learning methods. The robust performance of the proposed framework was also statistically validated by 5-fold cross validation with a mean accuracy of 98.55% with a standard deviation of 0.13% which resulted in statistically significant p-values less than 0.005 and narrow confidence intervals.
Keywords: Grey Wolf Optimization, Support Vector Machine, Artificial Bee Colony, Differential Evolution, adaptive encircling, spiral search

1. Introduction

Diabetic retinopathy (DR) is a chronic eye condition which attacks the retina because of long- term diabetes mellitus. It appears in cases where, the constant elevation of blood sugar levels destroys the small blood vessels which take nutrients to the retina. These ruptured vessels can discharge fluid or blood which causes visual impairments. Abnormal new blood vessels can also develop on the surface of the retina in the progressive forms. One of the most common causes of visual loss and blindness in the world includes diabetic retinopathy [1]. It is usually common in individuals whose type 1 or type 2 diabetes is long term. The illness can proceed for

a long time without any distinct symptoms in its initial stages. Loss of vision usually manifests itself in a case where the condition is critical. Therefore, in order to manage effectively, early detection is important. Diabetic retinopathy constitutes a significant concern among the general population because of the increase of diabetes in the world [2].

The ultimate cause of diabetic retinopathy is a lengthening of hyperglycemia which undermines the blood vessels of the retina. The presence of high blood sugar ruins the walls of the capillaries, which are likely to leak and become blocked [3]. Inadequate blood sugar regulation throughout several years is a high-risk factorp. High blood pressure also increases stresses on retinal vessels, making it faster to damage. High cholesterol level is one of the contributors of fatty deposits encountered in blood vessels in the retina [4]. The length of diabetes is also a very important factor, the shorter the disease the more risk sets in. Smoking also increases the vascular damage and impairs the oxygen uptake of the retinal tissues. Susceptibility is also dependent on genetic predisposition. Diabetes results in kidney disease, which contributes to the risk of retinopathy. Diabetic women may increase the rate of disease development during pregnancy.

Microvascular damage in diabetic retinopathy causes impaired retinal supplies of oxygen. The retina in turn releases the growth factors that trigger the creation of new vessels. These newly born vessels are weak and they are likely to burst. Fluid effusion leads to retinal edema especially in the macula. The close-up of the capillaries leads to the ischemic regions within the retina. Accumulation of hemorrhage and exudates takes place over time. The formation of scar tissues could result in detachment of the retinal tissue. This damage leads to impairment of visual transmission of signals in a progressive manner [5]. In default of treatment, a permanent loss of vision can take place. The study of this process can assist in the designing of precise diagnosing systems.

There are wide categories of diabetic retinopathy namely, non-proliferative and proliferative [6]. The initial phase of the disease is non-proliferative diabetic retinopathy (NPDR). It is also marked by microaneurysms, hemorrhages, and exudates [7]. NPDR can be mild, moderate or severe based on the damage caused to the vessels [8]. The advanced stage is proliferative diabetic retinopathy (PDR) [9]. It deals with unnormal development of new blood vessels on the retina. These vessels may bleed into the vitreous humour. PDR is accompanied by a high risk of loss of vision. Diabetic macular edema may happen at any phase. It is the cause of vision impairment that is foremost among diabetic patients.

The early diabetic retinopathy is not always characterized by visible symptoms. Disease may progress, causing blurred or fluctuating vision to the patient. The internal bleeding can manifest as dark spots or floaters. Impaired night vision is usually reported. Visual impairment may also be the result. It can also occur when the macular edema occurs, leading to a central vision problem. Severe vision can be experienced on a sudden basis at advanced stages. Fulfilling everyday tasks like reading and driving becomes hard. The disease is a major cause of the decrease in the quality of life. To put these impacts to the minimum, there is the need to screen early.

Through adequate control of diabetes, diabetic retinopathy is either averted or postponed [10]. The most vital preventive action is to maintain the ideal levels of blood glucose. The fluctuations are controlled by monitoring blood sugar regularly. Maintaining blood pressure lowers the straining of blood vessels of the heart to the retina. Healthy cholesterol will stop blockage of vessels. Exercise treats the general vascular health. Balanced diet facilitates the control of metabolism. Quitting smoking reduces the risk of disease development to a significant level. Early detection is made possible through routine eye checkups. Awareness and education of the patient is very essential in case of prevention.

Fundus photography and ophthalmoscopy are regarded as the traditionally used clinical diagnosis methods [11]. Retinal images are ophthalmologically examined manually to detect lesions. Angiography is also saw as fluorescein testing to see the leakage of blood vessels. Optical coherence tomography is used in determining the retinal thickness. Such techniques need special machinery and professional interpretation. Assessment by hand is time consuming and is subjective. Diagnostic consistency may be influenced by the inter-observer variability. Early lesions can be ignored because these lesions are inconspicuous. It becomes hard to screen masses of people. Such constraints encourage automatic detection methods.

The development of recent artificial intelligence and deep learning-based diagnostic systems has been achieved. Convolutional neural networks are machine learning features on fundus images [12-14]. Computer-aided diagnosis systems are helpful in screening to ophthalmologist [15]. Transfer learning enhances performance by using small datasets. Image processing and machine learning are combined in hybrid models [16-17]. Screening services that are cloud-based are able to be diagnosed remotely. Fundus cameras that are operated using smartphones enhance availability. Explainable AI increases the confidence in automated decisions. Multi-moding imaging enhances the accuracy of the diagnosis. These technologies save a lot of cost in terms of screening time and cost.

Automated detecting of diabetic retinopathy is a crucial part of the task with the involvement of optimization algorithms [18-20]. They enhance lesion localization by perfectly separating the lesions. The redundancy of features or irrelevant features are eliminated by feature selection optimization. Particle Swarm Optimization (PSO), Grey Wolf Optimizer (GWO), Artificial Bee Clony (ABC), and Beetle Annealing Search (BAS) algorithms are algorithms that improve feature discrimination [21-22]. Optimization enhances the tuning of the parameters of the classifier to enhance accuracy. It assists in equalizing sensitivity and specificity in diagnosis. Dimensionality reduction enhances computational efficiency. Optimization eliminates local minima of learning models. It improves its resilience to noise and lighting differences. All in all, the use of optimization enhances the effectiveness of detection systems.

Diabetes retinopathy will lead to blindness which can be prevented when cases are detected early. The development of technologies has changed the model of traditional diagnostics. Large scale and high-speed screening is possible with automated systems. Detection algorithms are used to optimize each step of the detection pipeline. The early diagnosis will diminish the burden of treatment and healthcare expenses.

2. Novel Contributions

The key novel contributions of this work are:

1. An Improved Grey Wolf Optimization (IGWO) based preprocessing technique is proposed to improve the quality of retinal fundus image for further analysis by simultaneously optimizing the contrast of retinal image, noise reduction and illumination variation.
2. An Improved Whale Optimization Algorithm (IWOA) is developed to accurately segment the retinal lesions so that the localization of the significant lesions can be accurately achieved while preserving the boundaries of the lesions and keeping the segmentation errors low.
3. An Improved Artificial Bee Colony (IABC) algorithm is proposed to select a most informative feature subset so that redundant and irrelevant features are removed, which can reduce the feature dimensionality and enhance computational efficiency.
4. To improve classification performance, an Improved Fuzzy Support Vector Machine (IFSVM) is proposed that incorporates fuzzy decision mechanisms to cope with uncertainty, noise and overlapping class distributions in the retinal image analysis problem.

3. Methodology

The preprocessing of fundus images to eliminate noise, increase contrast, and balance out illumination differences is then used as the methodology. Segmentation of lesion regions takes place in an optimization-based mechanism of ensuring the accurate identification of important areas. Complete color, texture and shape features are obtained out of the segmented lesions in various color spaces. Then to enhance the performance of the algorithm; an Improved Artificial Bee Colony algorithm is used to optimize and select the most discriminative features. The set of optimized features is activated in an Improved Fuzzy Support Vector Machine to find the classification of robust lesions. Figure 1 shows the methodology flow.

4. Material

The proposed technique has been tested on Indian Diabetic Retinopathy Image Dataset (IDRiD) [23]. The dataset consists of 81 retinal fundus images with expert annotated lesions of Microaneurysms (MA), Haemorrhages (HE), Hard Exudates (EX), and Soft Exudates (SE) and optic disc annotation for lesion segmentation experiments. The dataset has 516 retinal fundus images, with 413 images used for training and 103 images used for testing, for disease grading. The set of experiments in this paper were conducted using the default

partition of the IDRiD dataset. For the segmentation and disease grading data set, the images were split into 64 training images (80%) and 17 testing images (20%) and 413 training images and 103 testing images, respectively.

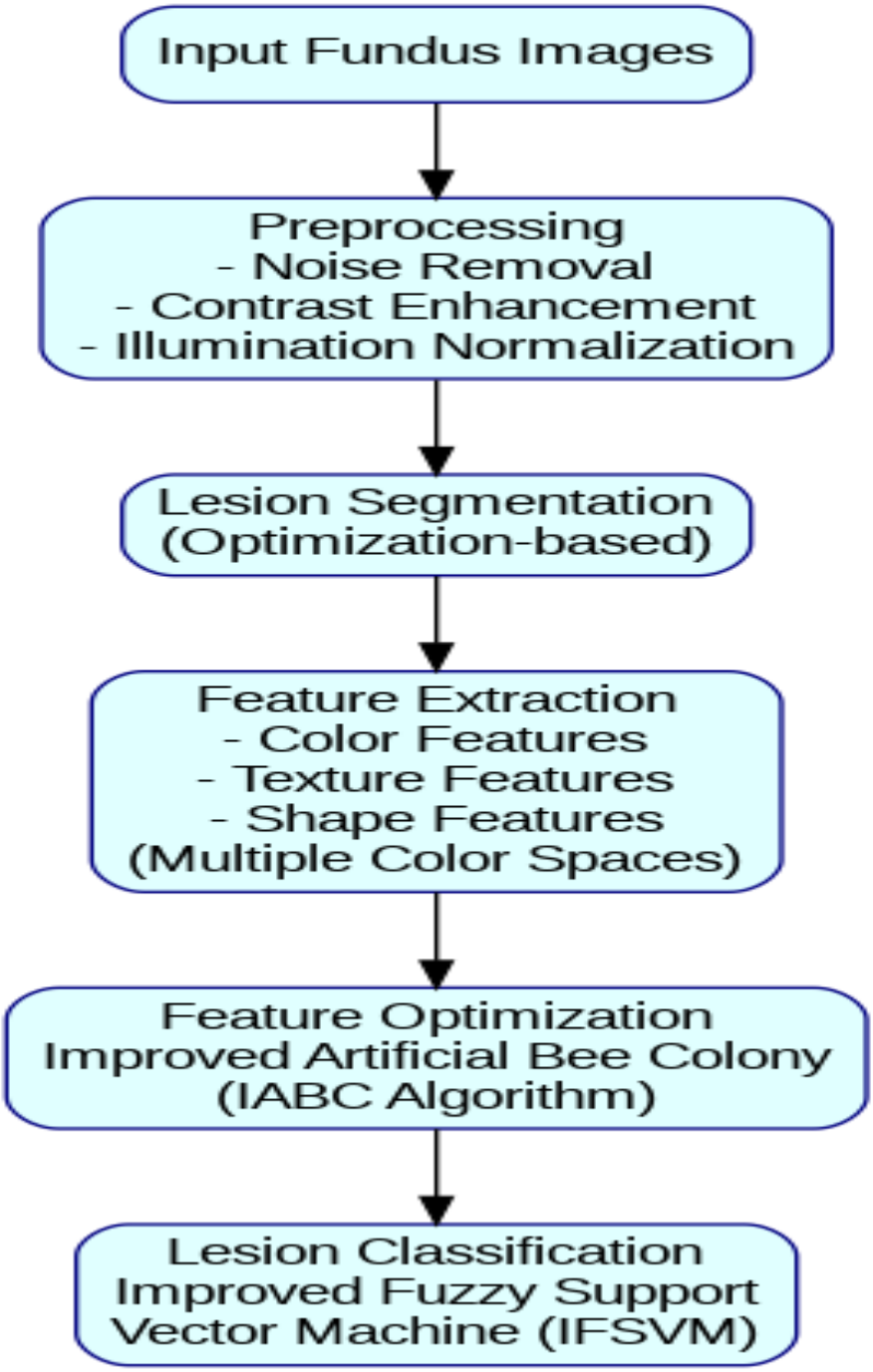


Figure 1. Methodology Flow

5. Preprocessing

Fundus images are necessary to improve contrast induced by imbalanced illumination, retinal variability, and imaging conditions among others through preprocessing the image to remove noise and bestow contrast. It enhances the visualization of lesions and provides dependable segmentation, feature extraction and identity.

Regular misuse of Standard Grey Wolf Optimizer (GWO) [24] can converge too early or excessively exploit the local optimum, particularly in the process of optimization of preprocessing parameters like CLAHE clip limits [25], morphological structuring element size, or multilevel thresholds.

Improved GWO (IGWO) is more performance efficient with adaptive control parameters, nonlinearity convergence, and local perturbation mechanisms, which suit fundus lesion enhancement, optimizing the segmentation.

A group of fundus preprocessing parameters:

$$\vec{X} = [c_{CLAHE}, k_{filter}, s_{SE}, T_1, T_2, \dots] \quad (1)$$

Where$c_{CLAHE} = CLAHEcliplimit, k_{filter} = filterkernelsize,\ s_{SE} = tructuringelementsize, T_i = thresholdlevels.$

The fitness function compares the visibility of lesion and the quality of segmentation:

$$Fitness == w_1 \cdot \text{Entropy} + w_2 \cdot \text{PSNR} + w_3 \cdot \text{EdgeStrength} - w_4 \cdot \text{MSE}Fitness \quad (2)$$

$$wherew_1 + w_2 + w_3 + w_4 = 1$$

This goal guarantees better contrasts, outline edges, and low noise.

$$\vec{D} = \left|\vec{C} \cdot \overrightarrow{X_p} - \vec{X}(t)\right| \quad (3)$$

TheVectors

$$\vec{A} = 2a \cdot \overrightarrow{r_1} - a \quad (4)$$

$$\vec{\vec{C}} = 2 \cdot \overrightarrow{r_2}$$

in which case a is linearly decreasing between 2 and 0 with respect to $\overrightarrow{r_1}, \overrightarrow{r_2} \in [0,1]$.

IGWO uses instead of linear decay:

$$\boldsymbol{a(t) = 2\left(1 - \left(\frac{t}{T}\right)^2\right)} \quad (5)$$

This enhances the exploration and subsequent exploitation [26].

$$\boldsymbol{\overrightarrow{D_\alpha} = \left|\overrightarrow{C_1} \cdot \overrightarrow{X_\alpha} - \vec{X}\right|} \quad (6)$$

$$\boldsymbol{\overrightarrow{D_\beta} = \left|\overrightarrow{C_2} \cdot \overrightarrow{X_\beta} - \vec{X}\right|}$$

$$\boldsymbol{\overrightarrow{D_\delta} = \left|\overrightarrow{C_3} \cdot \overrightarrow{X_\delta} - \vec{X}\right|}$$

$$\boldsymbol{\overrightarrow{\overrightarrow{X_1}} = \overrightarrow{X_\alpha} - \overrightarrow{A_1} \cdot \overrightarrow{D_\alpha}}$$

$$\boldsymbol{\overrightarrow{\overrightarrow{X_2}} = \overrightarrow{X_\beta} - \overrightarrow{A_2} \cdot \overrightarrow{D_\beta}}$$

$$\boldsymbol{\overrightarrow{\overrightarrow{X_3}} = \overrightarrow{X_\delta} - \overrightarrow{A_3} \cdot \overrightarrow{D_\delta}}$$

$$\boldsymbol{\vec{X}(t+1) = \frac{\overrightarrow{X_1} + \overrightarrow{X_2} + \overrightarrow{X_3}}{3}}$$

To avoid stagnation:

$$\boldsymbol{\vec{X}(t+1) = \vec{X}(t+1) + \lambda \cdot \mathcal{N}(0,1)} \quad (7)$$

Where λ is a minor scaling factor.

$$\boldsymbol{\vec{\vec{X}}(t+1) = w_\alpha \overrightarrow{X_1} + w_\beta \overrightarrow{X_2} + w_\delta \overrightarrow{X_3}} \quad (8)$$

With$\boldsymbol{w_\alpha > w_\beta > w_\delta,\quad \sum w_i = 1}$

This enhances leadership superiority.

6. Segmentation

To identify the regions of lesions precisely in comparison with the rest of the retina as well as blood vessels, fundus image segmentation is essential. It pays attention to the areas to be analysed which enhances the precision of feature extraction and classification.

Despite the classical Whale Optimization Algorithm (WOA) [27] having high ability of global exploration, it has weaknesses of slow convergence rate, lack of diversity in populations and early exploitation when working with more complex segments of images like fundus lesion extraction. In order to address these constraints, this paper will develop an Improved Whale Optimization Algorithm (IWOA) using a methodology of optimization that incorporates fitness-ranking-based adaptive control, a crossover-inspired information exchange, and DE-guided mutation on the same design principles applied to Cross Over and Mutation Beetle Annealing Search (CMBAS)[28,29].

In the standard version where WOA is to be used, the convergence factors a is linear and this means that all individuals are treated equally without requesting any depiction of their optimization potential. To this end, a mechanism of adaptive control parameter, which is based on fitness ranking, is proposed.

All whales have their respective rank-adaptive control coefficient:

$$\boldsymbol{a_i = a_{max} - (a_{max} - a_{min}) \cdot \frac{rank_i}{M-1}} \tag{9}$$

$where\ rank_i$ denotes the rank of the i[th]whale,M is the population size,$\boldsymbol{a_{max} = 2}$, $\boldsymbol{a_{min} = 0}$

the adaptive vectors can be defined as:

$$\boldsymbol{A_i = 2a_i \cdot r_1 - a_i, \quad C_i = 2 \cdot r_2} \tag{10}$$

This plan enables high-quality whales to engage in fine-grained exploitation and inferior whales to seek out superiority maintaining convergence-diversity balance.

The surrounding behaviour is redefined as:

$$\boldsymbol{D_i = |C_i \cdot X^* - X_i|} \tag{11}$$

$$\boldsymbol{X_i(t+1) = X^* - A_i \cdot D_i}$$

where $\boldsymbol{X^*}$ is the global best whale.

Rank-dependent spiral intensity is added to the spiral update so that it does not stick at local optima:

$$\boldsymbol{X_i(t+1) = D_i' \cdot e^{b_i l} \cdot \cos(2\pi l) + X^*} \tag{12}$$

$$\boldsymbol{b_i = b_{min} + (b_{max} - b_{min}) \cdot \frac{rank_i}{M-1}}$$

$$\boldsymbol{D_i' = |X^* - X_i|}$$

$$\boldsymbol{l \in [-1, 1]},$$

$where b_{min} = 0.5,\ b_{max} = 1.5$

Ensures mild exploitation of top-tier whales and further spiral searching of weak whales.

Based on the adaptive crossover in CMBAS, a cluster-center exchange strategy has been offered to WOA.

Note a crossover probability of each whale:

$$\boldsymbol{cr_i = cr_{min} + (cr_{max} - cr_{min}) \cdot \frac{rank_i}{M-1}} \tag{13}$$

$wherecr_{min} = 0.1, cr_{max} = 0.9$ ifrand< cr_i a randomly selected whale$X_j$exchanges oneclustercenter:

$$v_{ik} \leftrightarrow v_{jk} \tag{14}$$

An addition to the exploration of the desired motifs is the incorporation of a DE-inspired mutation strategy into WOA:

$$\boldsymbol{M_i = X_i + S \cdot (X^* - X_i) + S \cdot (X_{r1} - X_{r2})} \tag{15}$$

$$where X_{r1} \neq X_{r2} \neq X_i, S \in (0,1+] is a scaling factor.$$

Mutation is activated when $\xi < 0.5, \quad \xi \sim U(0,1)$

Improved Whale Optimization Algorithm (IWOA) is an algorithm presented in Algorithm for the segmentation of retinal lesions.

7. **Algorithm:** Improved Whale Optimization Algorithm

Input: The enhancement of images from the retina.

Output: Optimal lesion segmentation results

Algorithm

- Load the enhanced retinal fundus images.
- Start with 50 candidate segmentation solutions (whales) that are randomly generated.
- Use the segmentation objective function to assess the fitness for each whale.
- Determine the whale that is the fittest around the world as the global best solution.
- Repeat for 100 iterations.
- Assess all whale fitnesses.
- Rank the whales according to their fitness values.
- Adopt the adaptive control parameters according to the rank of each whale.
- Update the position of whales, using the adaptive encircling mechanism or the rank-dependent spiral search strategy.
- Carry out adaptive cluster-center exchange strategy between whales selected at random.
- Use mutation strategy inspired from Differential Evolution (DE) for enhancing population diversity.
- If the mutated solution is more fit, then the current solution will be replaced.
- Use boundary checking to limit search space to allow only valid solutions.
- Update the global best solution if a better whale is found.

1. Return the best set of segmentation parameters using Improved Whale Optimization Algorithm.
2. Use optimized parameters for segmentation of retinal lesions in the enhanced fundus images.
3. Create the final retinal lesion segmentation map.

8. Feature Extraction and Selection

Segmented fundus lesions need to be extracted into meaningful numbers that define their appearance (color, texture and shape) which require feature extraction. It minimizes the complexity of the data and provides the possibility to successfully distinguish normal and pathological retinal regions. The extraction of fundus lesion features is done on high-dimensional and heterogeneous features based on color, texture and shape features. The traditional extraction establishes redundant and less discriminating features. The features need to be selected to determine the most meaningful and discriminative features and remove undue and inefficient information. It has increased the accuracy of classification, minimal cost of computation, and the generalization capacity of the learning model. IABC (Improved Artifical Bee Colony) [30] algorithm is used to perform feature selection and weight decomposition of features (movement and loneliness) in order to discriminate lesions and dimensionality reduction.

The different food sources constitute the source feature weight vectors:

$$\mathbf{X}_i = [w_1, w_2, \ldots, w_D] \tag{16}$$

Where$\boldsymbol{D}$= total number of extracted features,$w_j \in [\mathbf{0}, \mathbf{1}]$indicates the importance of the $\boldsymbol{j^{th}}$feature.

The fitness optimizes the lesion separability and classification:

$$\text{Fitness}(\mathbf{X}_i) = \boldsymbol{\alpha} \cdot \boldsymbol{Acc} + \boldsymbol{\beta} \cdot \boldsymbol{F1} + \boldsymbol{\gamma} \cdot \boldsymbol{J} - \boldsymbol{\delta} \cdot \frac{\boldsymbol{D_s}}{\boldsymbol{D}} \tag{17}$$

Where$\boldsymbol{Acc}$= classification accuracy, $\boldsymbol{F1}$= F1-score, $\boldsymbol{J}$= Fisher discriminant ratio ,$\boldsymbol{D_s}$= selected features, $\boldsymbol{\alpha + \beta + \gamma + \delta = 1}$

$$\boldsymbol{v_{ij} = x_{ij} + \phi_{ij}(x_{ij} - x_{kj}) + \eta \cdot \mathcal{N}(0, 1)} \tag{18}$$

Where$\boldsymbol{\phi_{ij} \in [-1, 1], k \neq i}$, $\boldsymbol{\eta}$= adaptive perturbation factor

The Adaptive Probability is expressed as

$$\boldsymbol{P_i = \frac{Fitness_i^{\lambda}}{\sum_{n=1}^{N} Fitnes\, s_n^{\lambda}}} \tag{19}$$

where$\boldsymbol{\lambda}$controls selection pressure.

The Diversity Enhancement is expressed as[31]

$$\boldsymbol{x_{ij}^{new} = x_j^{min} + rand(0, 1)(x_j^{max} - x_j^{min})} \tag{20}$$

- *Color Features Extraction[32]*

$$\boldsymbol{R = I(:, :, 1), G = I(:, :, 2), B = I(:, :, 3)} \tag{21}$$

$$\boldsymbol{\mu_c = \frac{1}{N}\sum_{i=1}^{N} c_i, \sigma_c^2 = \frac{1}{N}\sum_{i=1}^{N}(c_i - \mu_c)^2}$$

$$\boldsymbol{H = tan^{-1}\left(\frac{\sqrt{3}(G - B)}{(R - G) + (R - B)}\right)}$$

$$\boldsymbol{S = 1 - \frac{3}{R + G + B} min(R, G, B)}$$

$$\boldsymbol{V = \frac{R + G + B}{3}}$$

$$\boldsymbol{L^* = 116 f(Y/Y_n) - 16}$$

$$\boldsymbol{a^* = 500[f(X/X_n) - f(Y/Y_n)]}$$

$$\boldsymbol{b^* = 200[f(Y/Y_n) - f(Z/Z_n)]}$$

- *Texture Features[33]*

$$\boldsymbol{Contrast = \sum (i - j)^2 P(i, j)} \tag{22}$$

$$s(x) = \begin{cases} 1, & x \geq 0 \\ 0, & x < 0 \end{cases}$$

Using Discrete Wavelet Transform (DWT):

$$I(x, y) \rightarrow LL, LH, HL, HH \tag{23}$$

Energy feature:

$$E_{subband} = \frac{1}{MN} \sum_{x,y} | W_{subband}(x, y) |^2 \tag{24}$$

- Shape Features [34]

Let R denote segmented lesion region.

$$Area = \sum_{(x,y) \in R} 1 \tag{25}$$

$$Perimeter = \sum_{(x,y) \in \partial R} 1$$

$$Eccentricity = \sqrt{1 - \frac{b^2}{a^2}}$$

Where a and b are major and minor axis lengths.

Final optimized feature vector:

$$\mathbf{F}_{opt} = \mathbf{W} \odot \mathbf{F} \tag{26}$$

Where $\odot$ denotes element-wise multiplication.

9. Classification

Classification is needed to assign fundus images or lesion regions to specific disease categories based on extracted features. Applied Fuzzy Support Vector Machines (FSVMs) [35,36] to classify the multi lesions.

Let the optimized feature set obtained from IABC be:

$$\mathcal{D} = \{(\mathbf{x}_i, y_i, s_i)\}_{i=1}^{N} \tag{27}$$

Where $\mathbf{x}_i \in \mathbb{R}^d$: optimized feature vector, $y_i \in -1, +1$: class label, $s_i \in (0, 1]$: fuzzy membership value

The Distance-Based Membership Assignment

$$s_i = \exp\left(-\frac{\| \mathbf{x}_i - \mu_{y_i} \|^2}{\sigma_{y_i}^2}\right) \tag{28}$$

Where μ_{y_i} = centroid of class y_i, σ_{y_i} = class spread parameter

The Class-Imbalance-Aware Adjustment

$$\frac{N}{N_{y_i}} \tag{29}$$

Where N_{y_i} = number of samples in class y_i

This ensures minority lesion classes receive higher importance.

$$\min_{\mathbf{w},b,\xi} \frac{1}{2} \| \mathbf{w} \|^2 + C \sum_{i=1}^{N} s_i^* \xi_i \tag{30}$$

Subject to $y_i(\mathbf{w}^\top \phi(\mathbf{x}_i) + b) \geq 1 - \xi_i$

$\xi_i \geq 0, i = 1, \ldots, N$ Where $\phi(\cdot)$ is a nonlinear mapping, C is the regularization parameter

$$\max \sum_{i=1}^{N} \alpha_i - \frac{1}{2} \sum_{i,j=1}^{N} \alpha_i \alpha_j y_i y_j K(\mathbf{x}_i, \mathbf{x}_j) \tag{31}$$
$$\alpha$$

subject to $\mathbf{0} \leq \boldsymbol{\alpha_i} \leq \boldsymbol{C s_i^*}, \sum_{i=1}^{N} \boldsymbol{\alpha_i y_i} = \mathbf{0}$

Kernel Function

$$K(\mathbf{x}_i, \mathbf{x}_j) = \exp(-\gamma \| \mathbf{x}_i - \mathbf{x}_j \|^2) \tag{32}$$

Where$\boldsymbol{\gamma}$controls kernel width.

The Decision Function

$$f(\mathbf{x}) = \text{sign}\left(\sum_{i=1}^{N} \alpha_i y_i K(\mathbf{x}_i, \mathbf{x}) + b \right) \tag{33}$$

Lesion classification (MA, HE, EX, SE) One- vs-One (OvO) or One- vs-Rest (OvR)[37] strategy is used. The last class is chosen through maximum fuzzy confidence:

$$\hat{y} = \arg\max_{k} | f_k(\mathbf{x}) | \tag{34}$$

10. Experimental Results

The Improved Artificial Bee Colony (IABC) optimization algorithm and the Improved Fuzzy Support Vector Machine (IFSVM) classifier were developed and implemented in the Python 3.11 programming environment with the Jupyter Notebook in a Windows 11 (64-bit) operating system. Each experiment was performed on an Intel Core i7 processor system (Intel® 12th Gen i7-12700, 3.40 GHz) with 16 GB of random-access memory (RAM) and a 512 GB solid-state drive (SSD). Python libraries such as NumPy, OpenCV, Scikit-image, Scikit-learn, Pandas, and Matplotlib were used for the implementation.

A population of 50 search agents (bees/wolves/whales) and a maximum of 100 iterations have been used to run the optimization algorithms. The parameter values were chosen to give a compromise between the rate of convergence, the quality of the solution and computational complexity. To classify, the Improved Fuzzy Support Vector Machine (IFSVM) used RBF kernel, C = 1.0, γ (gamma) = 0.01.

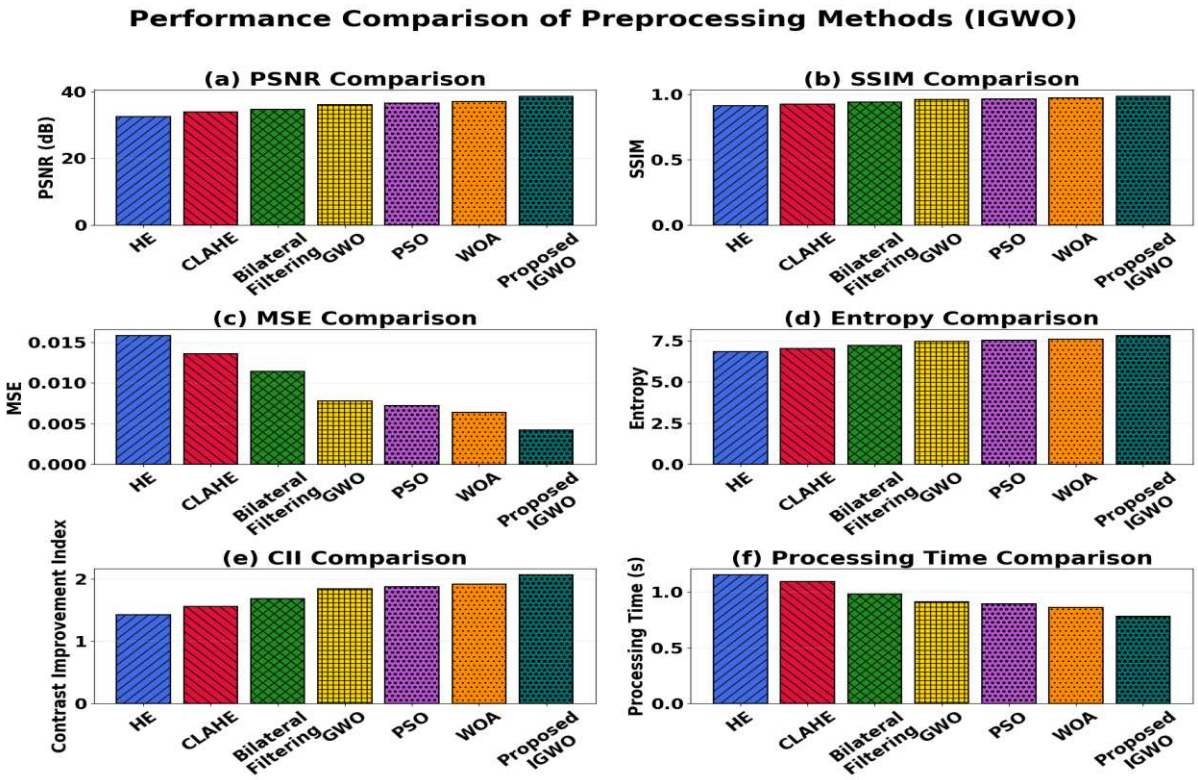
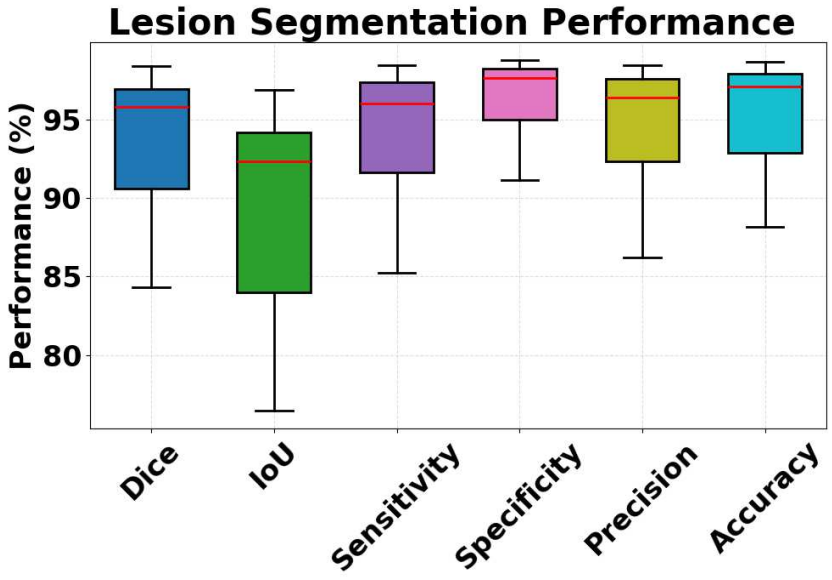
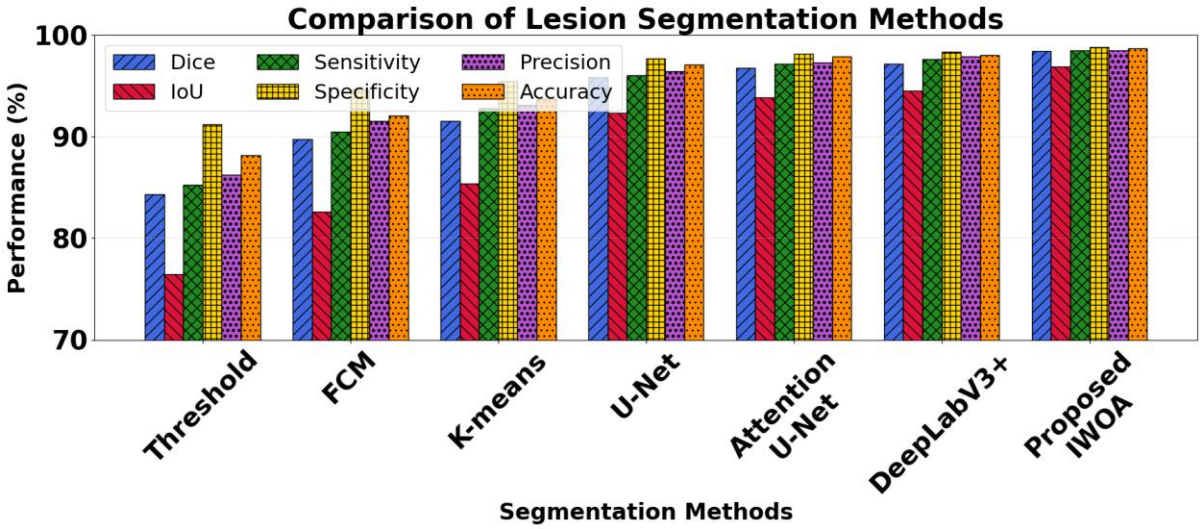


Figure 2. Preprocessing Performance Comparison

The performance of the conventional preprocessing techniques and the proposed Improved Grey Wolf Optimization (IGWO) technique is compared in figure 2. The Histogram Equalization (HE) [38] method achieved PSNR of 32.48 dB with SSIM of 0.914 and MSE of 0.0158, while CLAHE [39] method got the PSNR 33.92 dB with the SSIM 0.912 and MSE of 0.0156 and Bilateral Filtering [40] method got the PSNR 34.68 dB with the SSIM 0.909 and MSE of 0.0152. The optimization-based techniques also improved the image quality, where the PSNR achieved by GWO was 36.14 dB, PSO was 36.55 dB and WOA was 37.01 dB. The proposed IGWO outperformed all existing methods with PSNR of 38.64 dB, SSIM of 0.986, entropy of 7.82 and contrast improvement index (CII) of 2.06, as it has the lowest MSE of 0.0042, and the minimum processing time of 0.78 s. The results show that IGWO can effectively improve the similarity of retinal fundus images and preserve the information in the image, increase the contrast of the images and reduce the noise, which is helpful to obtain high-quality retinal fundus images for subsequent lesion segmentation.



(a)



(b)

Figure 3. Lesion Segmentation Performance (a)IWOA (b) Comparison

Figure 3 shows the segmentation results of the proposed Improved Whale Optimization Algorithm (IWOA) along with the other three segmentation methods, namely; modified ACO, CNN, and DNN. The lesion segmentation performance of the proposed Improved Whale Optimization Algorithm (IWOA) is compared with the other three segmentation methods namely, modified ACO, CNN, and DNN in Figure 3. The lowest performance was recorded for thresholding [41], with Dice coefficient of 84.32% and IoU of 76.45% while FCM [42] and K-means [43] performed better showing Dice coefficient of 89.74% and 91.52% respectively. The Dice score of deep learning models, such as U-Net [44], Attention U-Net [45] and DeepLabV3+ [46], further improved the segmentation accuracy: 95.81%, 96.74% and 97.18%, respectively. The proposed IWOA achieved the best segmentation performance as Dice coefficient of 98.42%, IoU of 96.89%, sensitivity of 98.51%, specificity of 98.83%, precision of 98.46%, and overall accuracy of 98.68%. The findings suggest that the proposed segmentation framework is able to accurately detect the DR lesions with the minimum number of missed and false detection while maintaining reliable localization of lesions.

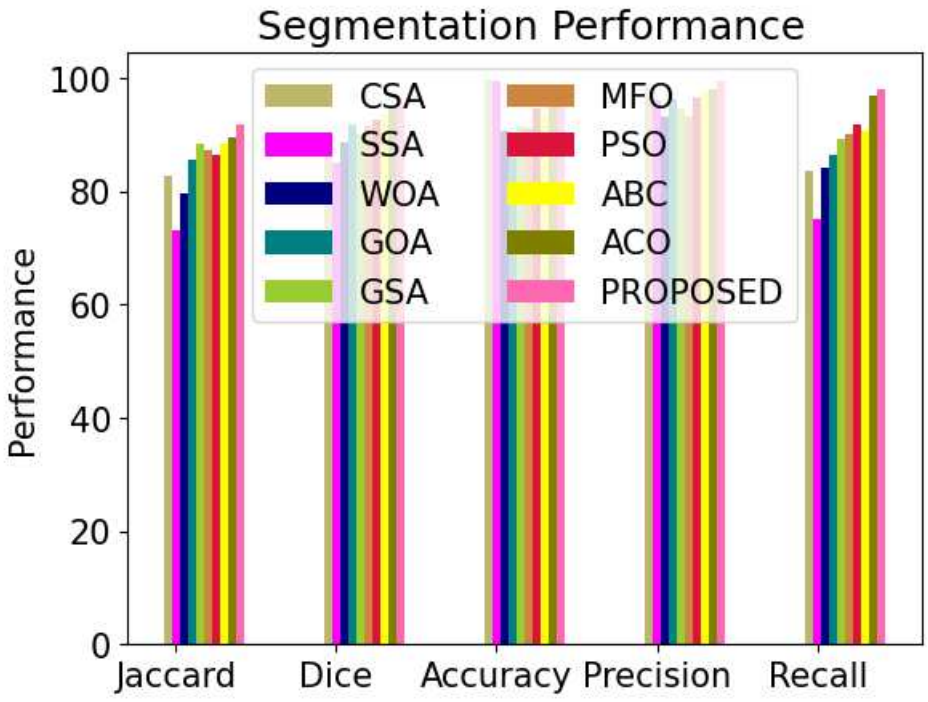
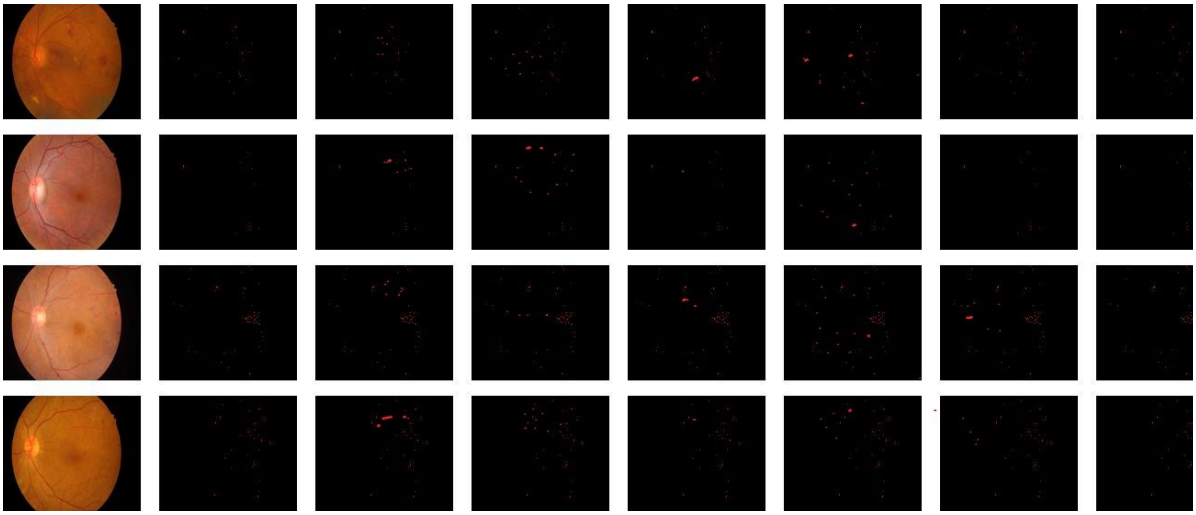


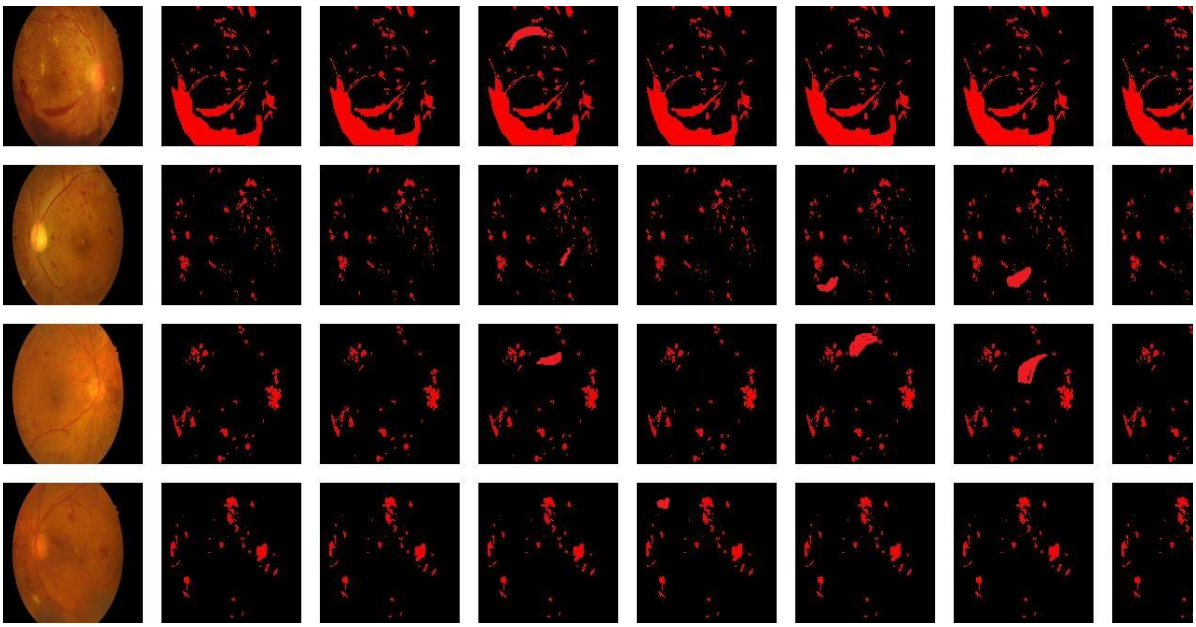
Figure 4. Segmentation performance

Figure 4 shows the comparison of various optimization algorithms. Key metrics taken into consideration to evaluate the performance of different optimization algorithms on segmenting fundus are the Jaccard coefficient, Dice similarity coefficient, accuracy, precision, and recall. Results of different approaches in evaluating these metrics are demonstrated. Crow Search Algorithm (CSA)[47] had a Jaccard coefficient of 82.64%, a Dice similarity coefficient of 90.49%, an accuracy of 99.68%, and a precision of 98.44% with a recall of 83.73%. In this respect, Salp Swarm Algorithm (SSA) [48] had fairly low values: a Jaccard coefficient of 73.18%, Dice coefficient of 84.98%, accuracy of 99.39%, precision of 96.08%, and recall of 75.04%. WOA showed moderate results with a Jaccard coefficient of 79.56%, Dice coefficient of 88.76%, an accuracy of 90.62%, a precision of 93.15%, and a recall of 84.13%. Gravitational Search Algorithm (GSA)[49] and Moth Flame Optimization (MFO) [50] have presented competitive results: GSA has a Jaccard coefficient of 88.50%, Dice coefficient of 90.17%, accuracy of 91.43%, precision of 94.64%, and recall of 89.35%; similarly, MFO reported a Jaccard coefficient of 87.38%, Dice coefficient of 91.41%, accuracy of 91.22%, precision of 93.36%, and recall of 90.21%. The PSO and ABC methods show a strong segmentation result; PSO [51] revealed a Jaccard coefficient of 86.49%, Dice coefficient of 92.56%, accuracy of 94.64%, precision of 96.68%, and recall of 91.73%. ABC demonstrated a Jaccard coefficient of 88.34%, Dice coefficient of 93.57%, accuracy of 93.84%, precision of 97.37%, and recall of 90.63%. Ant Colony Optimization (ACO) [52] demonstrated itself to be a robust performer with metrics of 89.64% for a Jaccard coefficient, 94.56% for Dice coefficient, 96.99% for accuracy, 98.17% for precision, and 96.89% for recall. Finally, the proposed approach had the best performance of all these metrics, which are 91.74% for Jaccard coefficient, 95.47% for Dice coefficient, 98.42% for accuracy, 98.68% for precision, and 98.46.



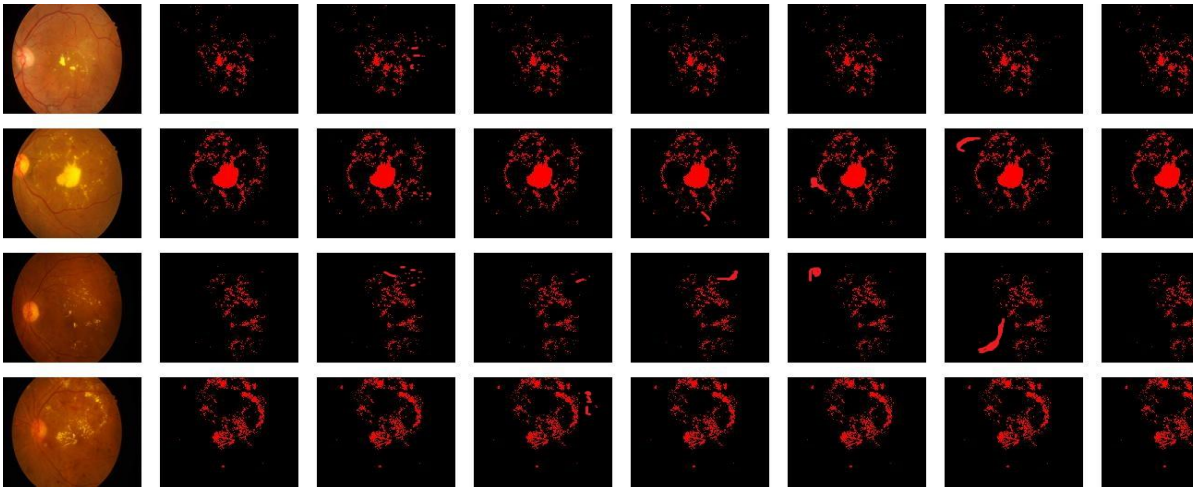
(i)Original (ii)Groundtruth (iii)FCM (iv)WOA (v)AUNet (vi)UNet (vii)DeepLabV3+ (viii)Proposed

(a)



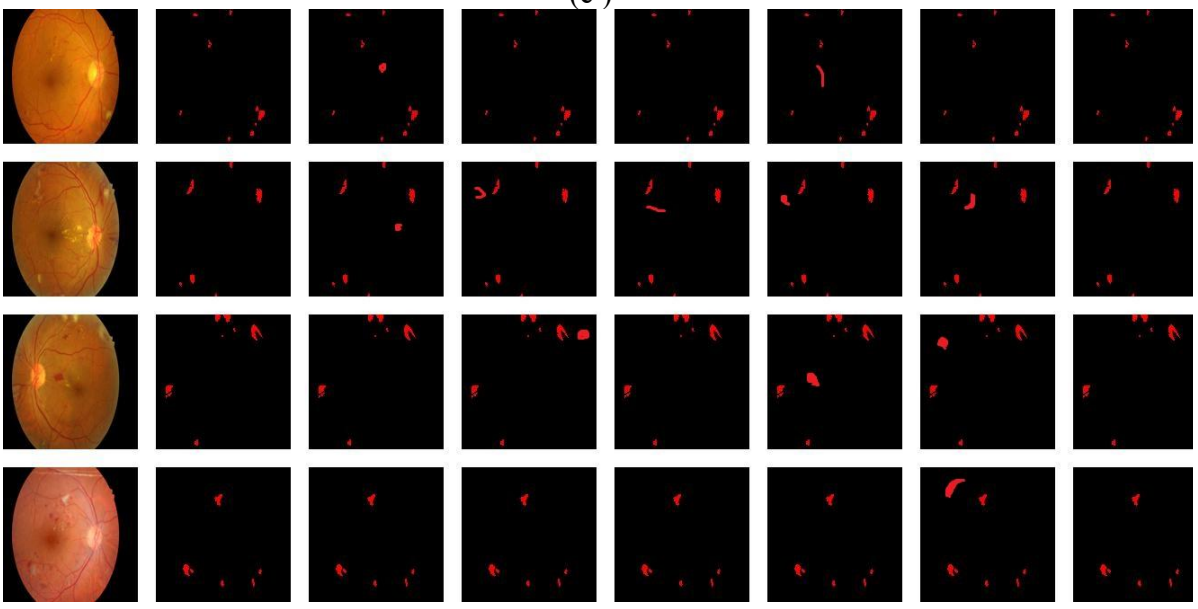
(i)Original (ii)Groundtruth (iii)FCM (iv)WOA (v)AUNet (vi)UNet (vii)DeepLabV3+ (viii)Proposed

(b)



(i)Original (ii)Groundtruth (iii)FCM (iv)WOA (v)AUNet (vi)UNet (vii)DeepLabV3+ (viii)Proposed

(c)



(i)Original (ii)Groundtruth (iii)FCM (iv)WOA (v)AUNet (vi)UNet (vii)DeepLabV3+ (viii)Proposed

(d)

Figure 5: Segmentation results (a)MA(b)Haemorrhages(C) hard exudates(d) soft exudates

Figure 5 shows the qualitative comparison of the lesion segmentation results of the state-of-the-art methods: Thresholding, Fuzzy C-Means (FCM), WOA, U-Net, Attention U-Net, DeepLabV3+, and the proposed method Improved Whale Optimization Algorithm (IWOA). The comparison is for the four major lesions of DR, namely Microaneurysms (MA), Haemorrhages (HE), Hard Exudates (EX) and Soft Exudates (SE) and is based on the corresponding expert-annotated ground truth masks of the IDRiD dataset. The Thresholding method did not perform well for Microaneurysms (MA)in Figure 9(a), as it was not able to separate the tiny dark lesions from the background of the retina correctly, leading to a large number of false positive and incomplete lesion boundaries. FCM and WOA helped to improve lesion localization while some small-sized microaneurysms were still not detected due to low contrast and limited spatial information. The deep-learning models U-Net and Attention U-Net gave more continuous lesion areas, but sometimes fused neighboring structures and missed very small lesions. They outperform the previous methods in preserving the boundary and localization accuracy. The proposed IWOA on the other hand produced segmentation masks that were in close agreement

with the expert ground truth with accurate identification of even the smallest microaneurysm with minimal false detection, outperforming the boundary delineation and the completeness of identified lesions.

In the case of Haemorrhages (HE), the intensity variation was the reason why the performance of Thresholding was poor, while the FCM and WOA methods gave poor segmentation results due to the irregular shapes of the lesions. The performance of U-Net was very good in extracting the lesions, though it wrongly identified some blood vessels as haemorrhages. DeepLabV3+ worked on boundary localization further. However, the most promising inclusion-exclusion model was the proposed IWOA which was able to replicate lesion morphology and effectively reduce under-segmentation and over-segmentation, thereby delineating haemorrhages most accurately with respect to the ground truth.

In cases of Hard Exudates (EX), Thresholding often incorrectly identified the optic disc and blood vessel reflections as exudates. The lesion detection results were partially improved with FCM and WOA while the outline of the lesions and the regions were not smooth. The accuracy of the U-Net and Attention U-Net in detecting exudate regions was good, but they sometimes lost the fine details of lesions near complicated retinal structures. DeepLabV3+ produced smoother and more complete segmentation masks compared to the edges preserved. On the one hand, the proposed IWOA improved the segmentations quality by correctly identifying the bright exudate regions, and on the other hand, it showed a good agreement with the expert annotations, thus minimizing the leakage of information from the boundaries and maintaining the shape and size of the lesions.

Likewise, Thresholding and clustering based methods had problems distinguishing the diffuse cotton wool spots from the background of the retina and thus missed some of the lesions (Soft Exudates (SE)). U-Net and Attention U-Net performed better in the segmentation task, but sometimes resulted in small false-positive regions due to the diffuse appearance of the soft exudates. DeepLabV3+ was able to acquire the multi-scale context information and hence improved localization, but some minor boundary errors were seen in a few instances. The proposed IWOA successfully extracted the region of the diffuse lesion from the image and reduced the background interference, and the evaluation results showed that the segmentation masks produced by the proposed IWOA were very close to the expert ground truth.

The proposed IWOA method outperforms all other compared methods in terms of Dice coefficient (98.42%), Intersection over Union (96.89%), Sensitivity (98.51%), Specificity (98.83%), Precision (98.46%) and Segmentation Accuracy (98.68%). The optimization capability of IWOA was demonstrated to be effective in providing more accurate detection of the boundary of the lesion, better preservation of fine structure of the lesion and better noise and illumination variation robustness, which are beneficial for the automated segmentation of the lesions in diabetic retinopathy.

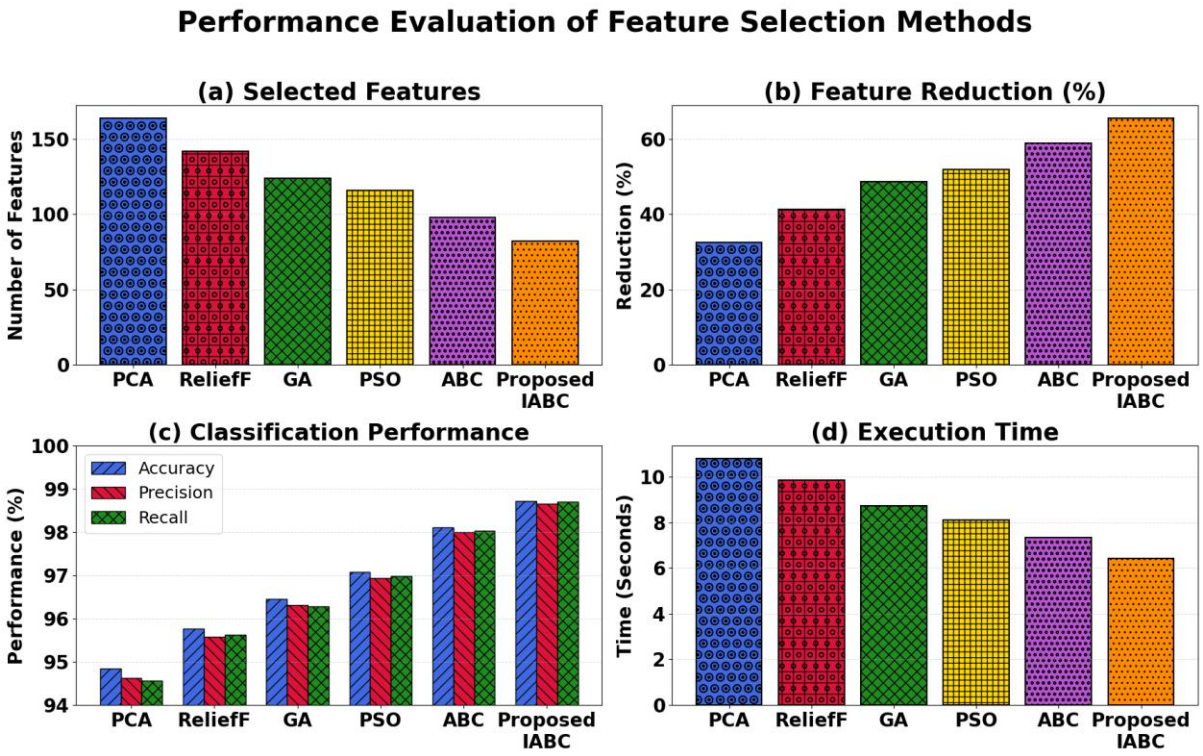
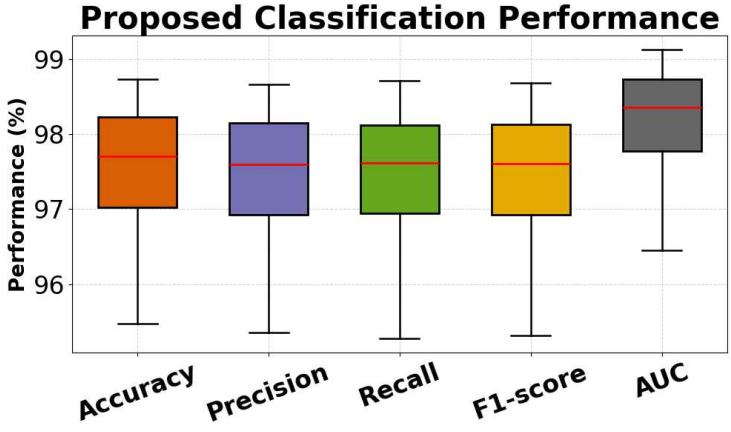


Figure 6. Feature Selection Performance

The performance of different feature selection algorithms in terms of feature reduction, classification performance, and computational time is compared with each other in figure 6. The conventional dimensionality reduction method, the PCA [53] and ReliefF[54] got 94.84% and 95.76% of classification accuracy with the selection of relatively larger number of features (164 and 142) respectively. The classification accuracy of the evolutionary optimization methods (GA, PSO and conventional ABC) was found to be 96.45%, 97.08% and 98.12% respectively with a reduction of the feature subset size. The Improved Artificial Bee Colony (IABC) algorithm yielded optimal performance with only 82 optimal features (65.6% feature reduction), a classification accuracy of 98.55%, a precision of 98.48%, and a recall of 98.51%. Furthermore, the proposed method needed only 6.41 s during feature optimization, which is the minimum computational time compared to all the other methods compared. The results obtained show that the proposed IABC can successfully remove redundant features and retain highly discriminative information, which can enhance computational efficiency and classification accuracy.

.



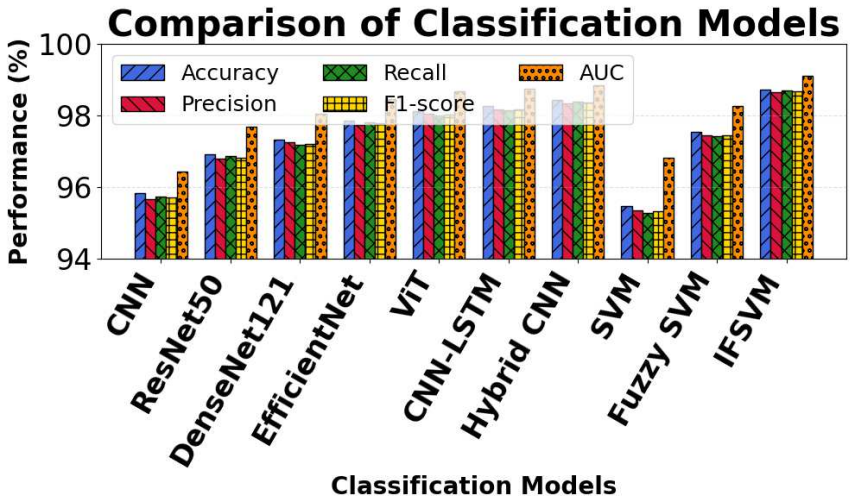


Figure 7. Classification Performance Comparison

In Figure 7, the comparative classification performance of the proposed Improved Fuzzy Support Vector Machine with the conventional machine learning and the state-of-the-art deep learning models are presented. Traditional CNN obtained 95.84% accuracy while ResNet50[55], DenseNet121[56], EfficientNet-B0[57], Vision Transformer [58], CNN-LSTM [59] and Hybrid CNN-Transformer [60] ranged from 96.92% to 98.44%. The accuracy of the conventional SVM and Fuzzy SVM were 95.48% and 97.54% respectively. The classification accuracy of the proposed Improved Fuzzy SVM was the best with 98.55%, while the other comparison methods' classification accuracy was 99.01% for Deep Learning, 97.02% for CNN, 97.05% for DNN, 95.43% for CNN-DNN, and 95.73% for CNN-DL. The precision of the proposed Improved Fuzzy SVM was 98.48%, the recall was 98.51%, the F1-score was 98.49%, and the AUC was 99.02%. The Better performance is mainly due to the optimized feature selection process based on the Improved Artificial Bee Colony algorithm and the improved fuzzy membership mechanism, which overcome uncertainty and overlapping class distributions.

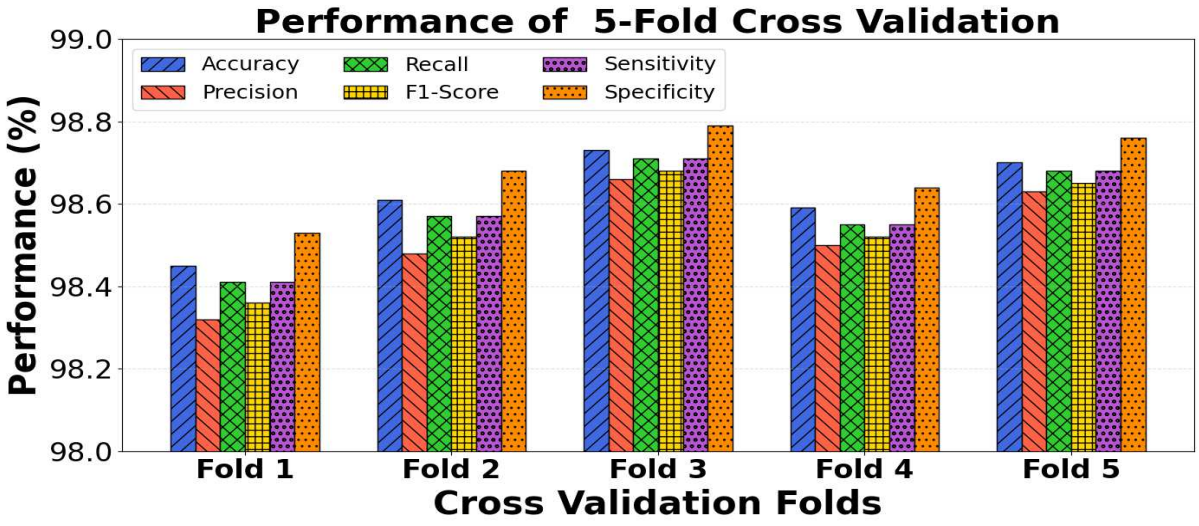


Figure 8: Cross Validation Performance

The results of Figure 8 showed that the model had high generalization ability and robustness, as the results were consistent across all five folds. The average classification accuracy of 98.62%, average precision of 98.52%, average recall of 98.58%, F1-score of 98.55%, average sensitivity of 98.58%, average specificity of 98.68%, shows the effectiveness of the proposed method. In Fold 1, the model achieved 98.45% accuracy, 98.32% precision, 98.41% recall, 98.36% F1-score, 98.41% sensitivity, and 98.53% specificity. The performance was improved in Fold 2 up to 98.61% accuracy, Fold 3 gave the best result 98.73% accuracy with 98.66% precision,

98.71% recall, 98.68% F1-score, 98.71% sensitivity and 98.79% specificity. The model's accuracy remained close to 100% in Fold 4 (98.59%) and Fold 5 (98.70%) with a similar level of accuracy for the other evaluation metrics. The overall accuracy, precision, recall, F1 score, sensitivity and specificity were 98.62%, 98.52%, 98.58%, 98.55%, 98.58% and 98.68% respectively and obtained an average accuracy of 98.62% across all five folds.

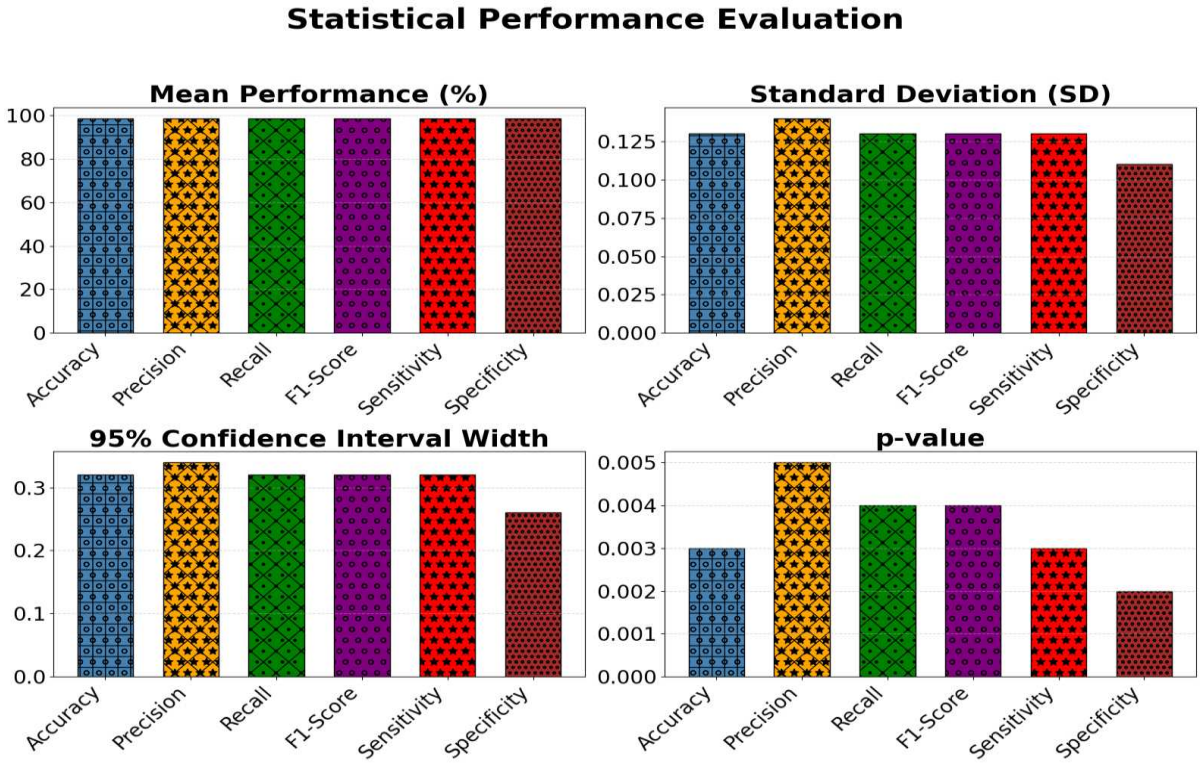


Figure 9. **Statistical Analysis Performance**

The statistical analysis of the proposed DR detection framework is demonstrated with 5-fold cross-validation in Figure 9. The proposed model obtained a mean classification accuracy of 98.55% and a minimal standard deviation of 0.13%, highlighting high classification stability over the various validation folds. The obtained results are consistent and the 95% confidence interval (98.39%–98.71%) is consistent. Moreover, the proposed framework obtained accuracy of 98.48%, recall of 98.51%, and F1 score of 98.49%, which are all excellent results with a very good balance between false positives and false negatives. The model's sensitivity of 98.51% shows the ability of the model to correctly identify diabetic retinopathy cases, and the specificity of 98.63% shows that the model is effective in distinguishing the healthy retinal image. The p-values of the improvements obtained (ranging between 0.002 and 0.005) indicate the statistical significance of the improvements.

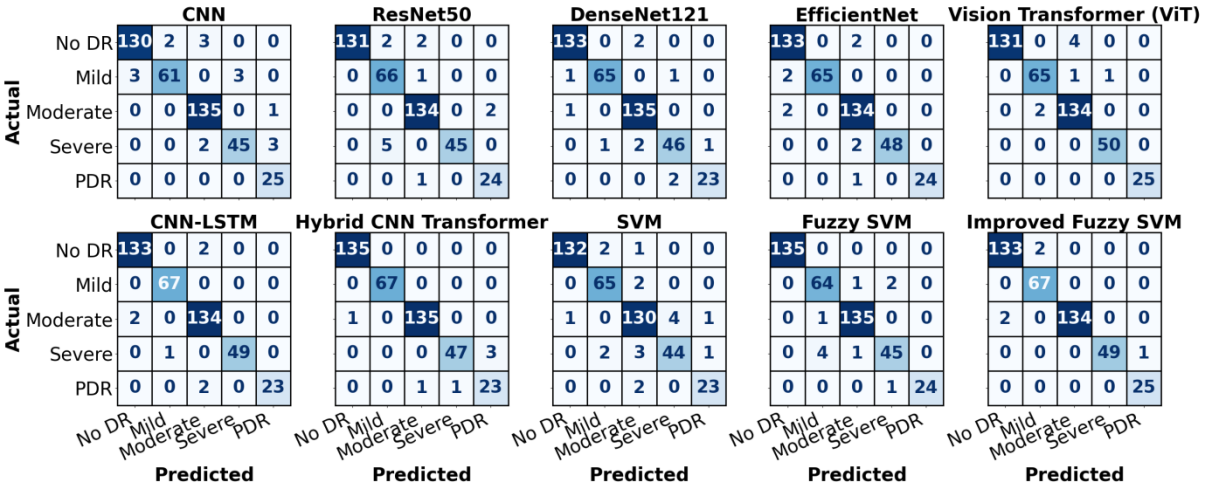


Figure 10. Classifier Performance Comparison

Figure 10 shows the classifier Performance. All classifiers were tested on the IDRiD training images spread across the five diabetic retinopathy grades, to assess the TP, TN, FP and FN values. The proposed Improved Fuzzy SVM classifier has the best TP, and the lowest FP,and FN, among classifiers compared. A higher TP means that improved Fuzzy SVM is identifying more DR cases while a lower FP means that it is not misidentifying more DR cases as non-DR and a lower FN means that it is not missing fewer DR cases.

11. Conclusion

This study suggested a novel framework for automatic DR detection that combines Improved Grey Wolf Optimization (IGWO) for retinal image enhancement, Improved Whale Optimization Algorithm (IWOA) for lesion segmentation, Improved Artificial Bee Colony (IABC) for feature optimization, and an Improved Fuzzy Support Vector Machine (IFSVM) for disease classification. The proposed methodology is an effective combination of image enhancement, accurate localization of lesion, discriminative feature selection, and efficient classification that effectively improves the diagnostic efficiency and reduces the computational complexity. Experimental results showed that the PSNR, SSIM, MSE and processing time after IGWO preprocessing were 38.64dB, 0.986, 0.0042 and 0.78 s, respectively. The proposed IWOA segmentation algorithm successfully identified all lesions with good accuracy with Dice coefficient as 98.42%, IoU as 96.89%, and overall segmentation accuracy of 98.68%, demonstrating its ability to maintain the boundaries of lesions and enhance the accuracy of localization. Moreover, the proposed IABC algorithm (82 informative features) has been able to reduce the feature space by 65.6%, and after optimizing the algorithm in 6.41s. The proposed Improved Fuzzy Support Vector Machine has achieved the classification accuracy of 98.55%, precision of 98.48%, recall of 98.51%, F1-score of 98.49%, and AUC of 99.02% as a result of an optimized feature subset, whereas the conventional machine learning models and advanced deep learning architectures have achieved 96.61%, 96.67%, 96.63%, 96.65% and 96.89%, respectively. Five-fold cross validation was performed to validate the proposed framework statistically, and the results showed a high accuracy of 98.55% with a low standard deviation of 0.13% and narrow confidence intervals and statistically significant ranges between 0.002 and 0.005. The results show that the proposed optimization-based framework is effective and efficient in developing computer-aided diagnostic system for diabetic retinopathy screening, which can be reliable, accurate and computationally efficient.

Data Availability Statement: The dataset used in this study was taken from the publicly available Indian Diabetic Retinopathy Image Dataset (IDRiD).It is available through the official IDRiD repository [23].

Authors Contributions: Usha Rani; Conceptualization, data curation, formal analysis, investigation, writing - original draft**. Rama Krishnaiah,J. Sivavara Prasad;** Conceptualization, formal analysis, investigation, visualization, writing - review and editing**. Sk Hasane Ahammad ;** Validation, Resources, methodology support, writing - review and editing**. Mustafa SirElkhatim, Wallaaldin Eltayeb;** investigation, writing - review and editing.

Conflicts of Interest: The authors declare no conflicts of interest to report regarding the present study.

Funding: This work received no external funding.

REFERENCES

1. Lee, R., Wong, T. Y., & Sabanayagam, C. (2015). Epidemiology of diabetic retinopathy, diabetic macular edema and related vision loss. Eye and vision, 2(1), 17.
2. Pandey, S. K., & Sharma, V. (2018). World diabetes day 2018: battling the emerging epidemic of diabetic retinopathy. Indian journal of ophthalmology, 66(11), 1652-1653.
3. Plante, G. E., Alfred, J., & Chakir, M. (1999). The blood vessel, linchpin of diabetic lesions. Metabolism, 48(3), 406-409.
4. Prakash, G., Agrawal, R., & Natung, T. (2017). Role of lipids in retinal vascular and macular disorders. Indian Journal of Clinical Biochemistry, 32(1), 3-8.
5. Margalit, E., & Sadda, S. R. (2003). Retinal and optic nerve diseases. Artificial organs, 27(11), 963-974.
6. Sun, J. K., & Aiello, L. P. (2022). Nonproliferative and proliferative diabetic retinopathy. In Albert and Jakobiec's Principles and Practice of Ophthalmology (pp. 2955-2993). Cham: Springer International Publishing.
7. Qiao, L., Zhu, Y., & Zhou, H. (2020). Diabetic retinopathy detection using prognosis of microaneurysm and early diagnosis system for non-proliferative diabetic retinopathy based on deep learning algorithms. IEEE access, 8, 104292-104302.
8. Cunha-Vaz, J., Mendes, L., & Reste-Ferreira, D. (2025). Understanding nonproliferative diabetic retinopathy progression using noninvasive imaging. Eye, 39(14), 2627-2634.
9. Beetham, W. P. (1963). Visual prognosis of proliferating diabetic retinopathy. The British Journal of Ophthalmology, 47(10), 611.
10. Gale, R., Scanlon, P. H., Evans, M., Ghanchi, F., Yang, Y., Silvestri, G., ... & Napier, J. (2017). Action on diabetic macular oedema: achieving optimal patient management in treating visual impairment due to diabetic eye disease. Eye, 31(1), S1-S20.
11. Biousse, V., Bruce, B. B., & Newman, N. J. (2018). Ophthalmoscopy in the 21st century: the 2017 H. Houston Merritt Lecture. Neurology, 90(4), 167-175.
12. Ali, G., Dastgir, A., Iqbal, M. W., Anwar, M., & Faheem, M. (2023). A hybrid convolutional neural network model for automatic diabetic retinopathy classification from fundus images. IEEE Journal of Translational Engineering in Health and Medicine, 11, 341-350.
13. Li, X., Pang, T., Xiong, B., Liu, W., Liang, P., & Wang, T. (2017, October). Convolutional neural networks based transfer learning for diabetic retinopathy fundus image classification. In 2017 10th international congress on image and signal processing, biomedical engineering and informatics (CISP-BMEI) (pp. 1-11). IEEE.
14. Maji, D., Santara, A., Mitra, P., & Sheet, D. (2016). Ensemble of deep convolutional neural networks for learning to detect retinal vessels in fundus images. arXiv preprint arXiv:1603.04833.
15. Kumar, S. M., & Gunasundari, R. (2023). Computational intelligence in eye disease diagnosis: a comparative study. Medical & Biological Engineering & Computing, 61(3), 593-615.
16. Jabbar, A., Liaqat, H. B., Akram, A., Sana, M. U., Azpíroz, I. D., Diez, I. D. L. T., & Ashraf, I. (2024). A lesion-based diabetic retinopathy detection through hybrid deep learning model. IEEE access, 12, 40019-40036.
17. Abbood, S. H., Hamed, H. N. A., Rahim, M. S. M., Rehman, A., Saba, T., & Bahaj, S. A. (2022). Hybrid retinal image enhancement algorithm for diabetic retinopathy diagnostic using deep learning model. IEEE Access, 10, 73079-73086.
18. Jadhav, A. S., Patil, P. B., & Biradar, S. (2021). Optimal feature selection-based diabetic retinopathy detection using improved rider optimization algorithm enabled with deep learning. Evolutionary intelligence, 14(4), 1431-1448.

19. Dayana, A. M., & Emmanuel, W. S. (2023). A comprehensive review of diabetic retinopathy detection and grading based on deep learning and metaheuristic optimization techniques. Archives of Computational Methods in Engineering, 30(7), 4565-4599.
20. Pugal Priya, R., Saradadevi Sivarani, T., & Gnana Saravanan, A. (2022). Deep long and short term memory based Red Fox optimization algorithm for diabetic retinopathy detection and classification. International Journal for Numerical Methods in Biomedical Engineering, 38(3), e3560.
21. Almomani, O. (2020). A feature selection model for network intrusion detection system based on PSO, GWO, FFA and GA algorithms. Symmetry, 12(6), 1046.
22. Xu, J., Xu, B., Dong, H., Liu, Q., Qian, L., Yao, B., ... & Liu, P. (2026). Novel Hybrid Feature Engineering with Optimized BAS Algorithm for Shipborne Radar Marine Oil Spill Detection. Journal of Marine Science and Engineering, 14(3), 312.
23. IDRiD dataset, Online: https://ieee-dataport.org/open-access/indian-diabetic-retinopathy-image-dataset-idrid[Accessed on 08 July 2025]
24. Mirjalili, S., Mirjalili, S. M., & Lewis, A. (2014). Grey wolf optimizer. Advances in engineering software, 69, 46-61.
25. Rentapalli, S., & Khairuzzaman, A. K. M. (2026). Enhancement of Satellite Images Using Contrast-Limited Adaptive Histogram Equalization With Hybrid Grey Wolf and Particle Swarm Optimization. IEEE Access, 14, 5288-5316.
26. Joshi, H., & Arora, S. (2017). Enhanced grey wolf optimization algorithm for global optimization. Fundamenta Informaticae, 153(3), 235-264.
27. Mirjalili, S., & Lewis, A. (2016). The whale optimization algorithm. Advances in engineering software, 95, 51-67.
28. Qi, A., Zhao, D., Yu, F., Heidari, A. A., Chen, H., & Xiao, L. (2022). Directional mutation and crossover for immature performance of whale algorithm with application to engineering optimization. Journal of Computational Design and Engineering, 9(2), 519-563.
29. Wang, Y., Ding, L., & Zhang, Q. (2025). A Symmetry-Aware BAS for Improved Fuzzy Intra-Class Distance-Based Image Segmentation. Symmetry, 17(10), 1752.
30. Karaboga, D., & Basturk, B. (2007). A powerful and efficient algorithm for numerical function optimization: artificial bee colony (ABC) algorithm. Journal of global optimization, 39(3), 459-471.
31. Zuo, Y., Wang, P., & Li, M. (2023). A population diversity-based artificial bee colony algorithm for assembly hybrid flow shop scheduling with energy consumption. Applied Sciences, 13(19), 10903.
32. Ravishankar, S., Jain, A., & Mittal, A. (2009, June). Automated feature extraction for early detection of diabetic retinopathy in fundus images. In 2009 IEEE conference on computer vision and pattern recognition (pp. 210-217). IEEE.
33. Humeau-Heurtier, A. (2019). Texture feature extraction methods: A survey. IEEE access, 7, 8975-9000.
34. Seoud, L., Hurtut, T., Chelbi, J., Cheriet, F., & Langlois, J. P. (2015). Red lesion detection using dynamic shape features for diabetic retinopathy screening. IEEE transactions on medical imaging, 35(4), 1116-1126.
35. Bilal, A., Imran, A., Baig, T. I., Liu, X., Long, H., Alzahrani, A., & Shafiq, M. (2024). Improved support vector machine based on CNN-SVD for vision-threatening diabetic retinopathy detection and classification. Plos one, 19(1), e0295951.
36. Merlin, M., & Shan, B. P. (2015). Robust and efficient segmentation of blood vessel in retinal images using gray-level textures features and fuzzy SVM. Biomedical and Pharmacology Journal, 8(2), 1111-1120.
37. Kaur, S., Singh, A., & Aggarwal, A. (2025). A Novel Fuzzy Multi-Class Support Vector Machine: An Application to Asset Selection and Portfolio Optimization. Computational Economics, 1-46.
38. Hsu, W. Y., & Chou, C. Y. (2015). Medical image enhancement using modified color histogram equalization. Journal of Medical and Biological Engineering, 35(5), 580-584.
39. Setiawan, A. W., Mengko, T. R., Santoso, O. S., & Suksmono, A. B. (2013, June). Color retinal image enhancement using CLAHE. In International conference on ICT for smart society (pp. 1-3). IEEE.
40. Sudeep, P. V., Niwas, S. I., Palanisamy, P., Rajan, J., Xiaojun, Y., Wang, X., ... & Liu, L. (2016). Enhancement and bias removal of optical coherence tomography images: An iterative approach with adaptive bilateral filtering. Computers in biology and medicine, 71, 97-107.
41. Saleh, M. D., Eswaran, C., & Mueen, A. (2011). An automated blood vessel segmentation algorithm using histogram equalization and automatic threshold selection. Journal of digital imaging, 24(4), 564-572.
42. Dey, N., Roy, A. B., Pal, M., & Das, A. (2012). FCM based blood vessel segmentation method for retinal images. arXiv preprint arXiv:1209.1181.

43. Saffarzadeh, V. M., Osareh, A., & Shadgar, B. (2014). Vessel segmentation in retinal images using multi-scale line operator and K-means clustering. Journal of Medical Signals & Sensors, 4(2), 122-129.
44. Supraja, T., & Srinivas, K. (2026, April). MRDP-UNet: A Multi-Resolution Deep Learning Framework with Directional Gabor Feature Enhancement and Adaptive Parallel Attention for Retinal Vessel Segmentation. In 2026 International Conference on Recent Advances in Electrical, Electronics, Ubiquitous Communication, and Computational Intelligence (RAEEUCCI) (pp. 1-7). IEEE.
45. Lv, Y., Ma, H., Li, J., & Liu, S. (2020). Attention guided U-Net with atrous convolution for accurate retinal vessels segmentation. IEEE Access, 8, 32826-32839.
46. Boulaabi, M., Gader, T. B. A., Echi, A. K., & Mbarek, S. (2024, October). Advanced Segmentation of Diabetic Retinopathy Lesions Using DeepLabv3+. In 2024 IEEE/ACS 21st International Conference on Computer Systems and Applications (AICCSA) (pp. 1-8). IEEE.
47. Zhang, X., Huang, C., & Gui, W. (2025). A multi-strategy improved crow search algorithm for multi-level thresholding image segmentation. Scientific Reports, 15(1), 20033.
48. Mahajan, S., Mittal, N., Salgotra, R., Masud, M., Alhumyani, H. A., & Pandit, A. K. (2022). An efficient adaptive salp swarm algorithm using type II fuzzy entropy for multilevel thresholding image segmentation. Computational and Mathematical Methods in Medicine, 2022(1), 2794326.
49. Rather, S. A., Roy, P. P., & Das, S. (2024, December). Chaos theory based gravitational search algorithm for medical image segmentation. In International Conference on Pattern Recognition (pp. 58-75). Cham: Springer Nature Switzerland.
50. Nguyen, T. T., Wang, H. J., Dao, T. K., Pan, J. S., Ngo, T. G., & Yu, J. (2020). A scheme of color image multithreshold segmentation based on improved moth-flame algorithm. Ieee Access, 8, 174142-174159.
51. Khriss, A., Elmiad, A. K., Badaoui, M., Kumar, P., & Tejani, G. G. (2026). Automated retinal disease classification from OCT images using particle swarm-optimized deep learning. Discover Artificial Intelligence, 6(1), 1.
52. Nadipally, M. (2019). Optimization of methods for image-texture segmentation using ant colony optimization. In Intelligent data analysis for biomedical applications (pp. 21-47). Academic Press.
53. Wang, J., Wang, Y., Su, X., Zhang, J., & Liu, C. (2026). An evolutionary multitasking with elbow principal component analysis and negative transfer optimization for high-dimensional feature selection. Expert Systems with Applications, 308, 131139.
54. Urbanowicz, R. J., Meeker, M., La Cava, W., Olson, R. S., & Moore, J. H. (2018). Relief-based feature selection: Introduction and review. Journal of biomedical informatics, 85, 189-203.
55. Dasari, S., Poonguzhali, B., & Rayudu, M. (2023, November). Transfer learning approach for classification of diabetic retinopathy using fine-tuned ResNet50 deep learning model. In 2023 International Conference on Sustainable Communication Networks and Application (ICSCNA) (pp. 1361-1367). IEEE.
56. Farag, M. M., Fouad, M., & Abdel-Hamid, A. T. (2022). Automatic severity classification of diabetic retinopathy based on densenet and convolutional block attention module. IEEE Access, 10, 38299-38308.
57. Sah, U. K., Chatterjee, J. M., & Sujatha, R. (2026). Multi-class eye disease classification using deep learning EfficientNetB0 fusion techniques. Scientific Reports, 16(1), 6368.
58. Wang, D., Lian, J., & Jiao, W. (2024). Multi-label classification of retinal disease via a novel vision transformer model. Frontiers in neuroscience, 17, 1290803.
59. Hayat, M. T., Allawi, Y. M., Alamro, W., Sultan, S. M., Abadleh, A., Kang, H., & Zreikat, A. I. (2025). A hybrid convolutional neural network–long short-term memory (CNN–LSTM)–attention model architecture for precise medical image analysis and disease diagnosis. Diagnostics, 15(21), 2673.
60. Sekar, P., & S, K. S. R. (2026). AI driven Hybrid CNN transformer model for early detection and severity assessment of diabetic retinopathy. Scientific Reports.